

Control for Passing Through Critical Speeds of an Energy Storage Flywheel System by Bias Current Control*

Yajun Zhang and Nobuyuki Kobayashi

Department of Mechanical Engineering, College of Science and Engineering,
Aoyama Gakuin University

5-10-1 Fuchinobe Sagami-hara Kanagawa, 229-8558, Japan
zhyajun@me.aoyama.ac.jp kobanobu@me.aoyama.ac.jp

Abstract—In this paper, we address a new method of switching the critical speed by control the bias current of magnetic bearing. The bias is changeable in the sense that is a function of the rotational speed, and varies on-line in a manner that the critical speed of the rotor is controlled far away from the rotational speed of the rotor. The total stiffness of system is switched with the additional stiffness, the critical speed is switched also. In order to demonstrate the validity of the proposed method, the method is applied to a 10MWh class energy storage flywheel system to realize the control of passing through critical speed in the range of control. A simulation study illustrates the performance of the proposed bias current control method is validity for control of passing through the critical of magnetic bearing systems.

Index Terms—Passing through critical speed, Bias current control, Energy storage, Flywheel system.

I. INTRODUCTION

The magnetic bearing is widely used in the energy storage system, which store rotating kinetic energy by heavy spinning disk, is more promising as energy storage devices than lead batteries, because of their longer machine life and higher performance. The contact-free rotation of flywheel system is realized by magnetic bearing. In order to raise the energy storage density, the operating speed is set higher than the first flexible mode. The energy is storied into a flywheel when the flywheel is accelerated. And the energy is extracted from the flywheel when the flywheel is decelerated. The energy storage flywheel system frequently passes through its critical speed in the range of control when the energy is storied in or extracted from the flywheel. Ordinarily, the magnetic bearing system is operated by inputting a fixed electric current in each electromagnet, which is called bias current. The bias current is used in magnetic bearing system in order to linearize the magnetic force. The linear control theory is applied to the linearized model for controller design.

In recent years, in order to design a low power consumption active magnetic bearing (AMB) system, control approaches have been developed with zero bias or low bias current. The zero-power control method was proposed by Nonami et al. [1]. For this method, an energy-saving active magnetic bearing was constructed, in which a permanent

magnet and an electromagnet are united. In this system, the attractive force of the bias currents in the conventional AMB system was replaced by a control force. Regarding the zero power control of an energy storage flywheel, the H_∞ control of a rigid rotor system without the gyroscopic effect was also studied by Sivrioglu and coworkers [2]. N.Motee and Queiroz realized a control based switch bias to reduce the power loss [3]. Those papers are designed controllers with small bias current, but do not use the bias current more actively.

This paper proposes a new method of switch the critical speed of the energy storage flywheel system by the control of the additional stiffness. The additional stiffness is the stiffness of the bias current in the magnetic bearing of a flywheel system. When the rotational speed is getting close to the critical speed, the bias current control is set to on. The critical speed is changed by the additional stiffness that is controlled by the bias current in the magnetic bearing. When the rotational speed passed through the critical speed, the bias current control is set to off. The additional stiffness and the critical speed return to the original value. In order to demonstrate the validity of this method, a 10MWh class energy storage flywheel system is used in this paper. The additional stiffness of the bias current, the control of passing through the flexible critical speed of the 10MWh class energy storage flywheel system in the range of control are given in this paper. From simulation results, it had been verified that the proposed method is useful for passing through the critical speed of energy storage flywheel systems.

II. BIAS CONTROL OF MAGNETIC BEARING

A. Additional stiffness of bias current

A simple magnetic bearing with two magnets is given in Fig.1.

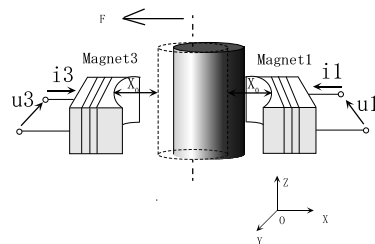


Fig. 1. Magnetic force

* This work is supported by ministry of education, culture, sports, science and technology of Japan from 2005. The number of the research is 17760188.

Flux density is given in (1).

$$H = \frac{\mu_0 n i}{2(x_0 - x_u)} \quad (1)$$

The magnetic force created by the magnet 1 in Fig.1 is given in (2).

$$F_1 = \frac{H^2 S}{\mu_0} = \frac{\mu_0 n^2 i^2 S}{4(x_0 - x_u)^2} \quad (2)$$

Equation (3) is gotten by substitute (1) into (2).

$$F_1 = \frac{\mu_0^2 S^2}{4(x_0 - x_u)^2} \frac{n^2 i^2}{\mu_0} = k \frac{i^2}{(x_0 - x_u)^2} \quad (3)$$

Here,

$$k = \frac{\mu_0 S n^2}{4} \quad (4)$$

μ_0 is the air permeability, n is the number of coils turns, x_0 is the nonminal air gap, x_u is the displacement and S is the pole area of the magnet. The bias current (i_{10}) and the control current (i_1) are included in i of (3).

Equation (5) is gotten by separate the bias and the control current in (3).

$$F_1 = k \frac{(i_{10} + i_1)^2}{(x_0 - x_u)^2} \quad (5)$$

Equation (6) is gotten by differentiate (5) with respect to i_1 .

$$\frac{\partial F_1}{\partial i_1} = \frac{2k(i_{10} + i_1)}{(x_0 - x_u)^2} \quad (6)$$

Equation (7) is gotten by differentiate (5) with respect to x_u .

$$\frac{\partial F_1}{\partial x_u} = \frac{2k(i_{10} + i_1)^2}{(x_0 - x_u)^3} \quad (7)$$

Equation (5) is linearized at $i_1 = 0$ and $x_u = 0$ by taylor expansion, (8) is gotten.

$$\begin{aligned} F_1 &= \left. \frac{\partial F}{\partial x_u} \right|_{i_1=0, x_u=0} x_u + \left. \frac{\partial F}{\partial i_1} \right|_{i_1=0, x_u=0} i_1 \\ &= \frac{2k(i_{10} + i_1)^2}{(x_0 - x_u)^3} \Big|_{i_1=0, x_u=0} x_u + \frac{2k(i_{10} + i_1)}{(x_0 - x_u)^2} \Big|_{i_1=0, x_u=0} i_1 \\ &= \frac{2k i_{10}^2}{x_0^3} x + \frac{2k i_{10}}{x_0^2} i_1 \end{aligned} \quad (8)$$

The resultant force of a pair of magnetic bearing, the magnet 1 and magnet 3, is the difference of the two magnetic forces.

$$F_{ux} = F_1 - F_3 = k \left[\frac{(i_{10} + i_1)^2}{(x_0 - x_u)^2} - \frac{(i_{30} - i_3)^2}{(x_0 + x_u)^2} \right] \quad (9)$$

Equation (9) is linearized using (8), and (10) is gotten.

$$F_{ux} = K_{bu} x_u + K_{cu} \quad (10)$$

Here,

$$K_{bu} = \frac{2k(i_{10}^2 + i_{30}^2)}{x_0^3} \quad K_{cu} = \frac{2k(i_{10} i_1 + i_{30} i_3)}{x_0^2}$$

From (10), the additive stiffness is controlled by the bias current. The stiffness of the system is affected by the additional stiffness. That is to say, the critical speed of the system is affected by the bias current.

B. Parameters of control model subjected to bias current

In order to switch the critical speed of the system, two sets of bias current are prepared, an original value and a critical speed value. Corresponding to the two sets of bias current, two models are designed. The two models have the same structure, but different stiffness matrix. The model with the original bias value is named model I, and the other model with the critical speed bias value is named model II. According to the different bias currents, the additional stiffness of the system, or the flexible critical speed of the system is switched between the two values. The parameter of the model is decided by the bias current inputted to the system.

C. Switching of two bias currents

The controller used for suspension and rotational is designed by the model I, and the system is controlled by this controller normally. The bias input is controlled by a ‘‘on-off’’ controller. When the rotational speed is getting close to the critical speed, the bias control is set to ‘‘on’’. The system is changed form model I to model II. The critical speed is shifted far away from the original place. And after the rotational speed passed through the original value of the critical speed, the bias control is set to ‘‘off’’, the critical speed returns to the original value. By this method, the control of passing through critical speed is realized and the system can be manipulated just like without passing through critical speed.

From the next section, the proposed method is applied to a 10MWh class energy storage flywheel system to verify the validity of the method.

III. SIMULATION SYSTEM

A. 10MWh class flywheel system

A 10MWh class superconducting magnetic flywheel system for electric power storage is shown in Fig.2 as a right-half cross-sectional view [4].

The positions of AMB1, AMB2, AMB3, superconducting magnetic bearing (SMB) and flywheel are shown in Fig.2. The total weight of the whole flywheel system is about 107t and the height is 6.86m. The weight of the flywheel is approximately 45.7t and the diameter is 4.8m. SMB is used to lift off the flywheel. In this system, SMB is applied to both of the axial direction and the radial direction.

In this paper, we only consider the active control of the radial direction by AMB. The flywheel system is suspended along the axial direction by a thrust bearing, positioned at the upper end of the system. The operational rotational speed of the flywheel is 6000rpm. To reinforce the material of flywheel at the maximum speed of system, the material of CFRP is applied.

B. FEM model

The vibration analysis of the rotational part by ANSYS is done to confirm there is a flexible mode in the range of control. The model of the rotational part used for controller

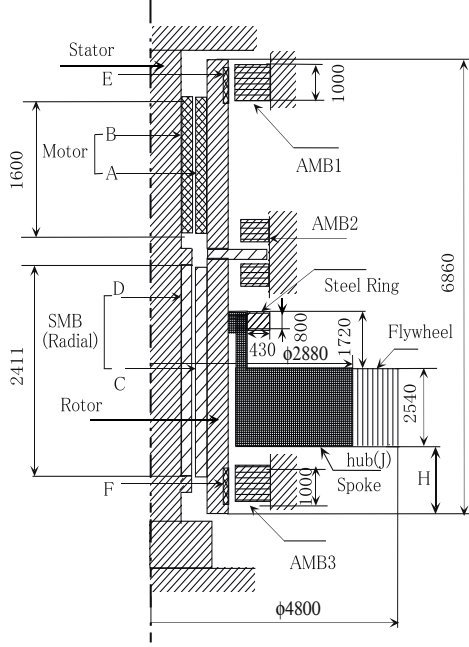


Fig. 2. Cross sectional view of flywheel system

design is constructed from the three dimensional model of ANSYS. While matching the parameters such as the total mass, the total height, the natural frequencies and the natural modes, the control model is designed. The rotor is divided into ten parts in solid line of Fig.3, and two parts in dashed line of Fig.3. The positions of the upper AMB, the below AMB, the motor and the flywheel are shown in Fig.3. $x_1, x_2, x_3, \dots, x_{12}, x_{22}, x_{32}$ are the displacements of each position, respectively. A one dimensional finite element method (FEM) model is designed and used in simulation based on two parts FEM model.

Based on Fig.3, the state equation and the output equation of the two divided FEM model are derived. Suppose the motion of the x direction is same to that of the y direction, only the x direction is considered. The motion of equation of the free-free flexible rotor system is given in (11). The damping effect is neglected.

$$\mathbf{M}_2 \ddot{\mathbf{Q}}_2 + \mathbf{K}_2 \mathbf{Q}_2 = \mathbf{B}_2 \mathbf{U}_2 \quad (11)$$

Here, \mathbf{M} is the mass matrix, $\mathbf{M} \in R^{6 \times 6}$. \mathbf{K} is the stiffness matrix, $\mathbf{K} \in R^{6 \times 6}$.

$$\mathbf{Q}_2 = [x_{12}, \theta_{x_{12}}, x_{22}, \theta_{x_{22}}, x_{32}, \theta_{x_{32}}]^T, \quad (12)$$

$$\mathbf{B}_2 = \begin{bmatrix} 1 & 0 & 0 & 0 & 0 & 0 \\ 0 & 0 & 0 & 0 & 1 & 0 \end{bmatrix}^T, \quad (13)$$

$$\mathbf{U}_2 = [F_{ux} \quad F_{lx}]^T. \quad (14)$$

F_{ux} is control input of upper magnetic electromagnet in x direction given in (10). F_{lx} is the control input of the below magnetic bearing in x direction as shown in (15).

$$F_{lx} = K_{bl}x_l + K_{cl} \quad (15)$$

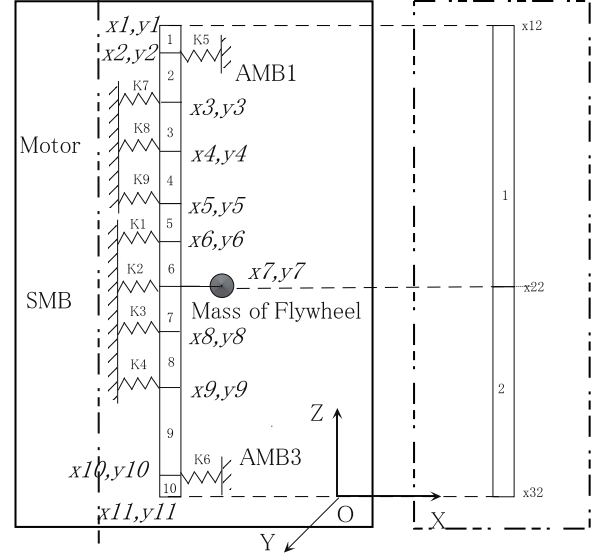


Fig. 3. FEM model

Here,

$$K_{bl} = \frac{2k(i_{10}^2 + i_{30}^2)}{x_0^3} \quad K_{cl} = \frac{2k(i_{10}i_{11} + i_{30}i_{31})}{x_0^2}$$

By substitute (10) and (15) into (11), (16) is gotten.

$$\mathbf{M}_2 \ddot{\mathbf{Q}}_2 + \mathbf{K} \mathbf{Q}_2 = \mathbf{B}_2 \begin{bmatrix} K_{cu} \\ K_{cl} \end{bmatrix} \quad (16)$$

Here, $x_u = x_{12}$ and $x_l = x_{32}$. The effects of K_{bu} and K_{bl} are considered in (16). This are the effects of the bias currents, used as additional stiffness. From (16), we see the stiffness of the system is subjected to the values of the bias current. The critical speed is moved by different bias currents also.

IV. CONTROLLER DESIGN

A. LQR control

In this paper, the optimal Linear Quadratic Regulator (LQR) control is applied to the FEM model to verify the proposed method. The objective is to find a control function \mathbf{u} to stabilize the system. A system is stabilizeable if there exists a state feedback control $\mathbf{u} = \mathbf{K}\mathbf{x}$ such that the closed loop system is exponentially stable. If the system is stabilizeable, then the LQR problem has a solution. The equation of a linear system is given in (17).

$$\begin{cases} \dot{\mathbf{x}}(t) = \mathbf{A}\mathbf{x}(t) + \mathbf{B}\mathbf{u}(t) \\ \mathbf{x}(0) = \mathbf{x}_0 \end{cases} \quad (17)$$

We want to find the control input $\mathbf{u}(t)$ as given in (18) and lead to the closed loop system given in (19) is exponentially stable.

$$\mathbf{u}(t) = -\mathbf{K}\mathbf{x}(t) \quad (18)$$

$$\dot{\mathbf{x}}(t) = (\mathbf{A} - \mathbf{B}\mathbf{K})\mathbf{x}(t) \quad (19)$$

One way of finding \mathbf{K} is by using *LQR* design. We seek a control input $\mathbf{u}(t)$ that minimizes the performance measure given in (20).

$$J = \int_0^{\infty} [\mathbf{x}(t)\mathbf{Q}\mathbf{x}(t) + \mathbf{u}(t)\mathbf{Q}\mathbf{u}(t)]dt \quad (20)$$

Where $\mathbf{x}(t)$ is the state of (17). $\mathbf{Q} = \mathbf{Q}^T \geq 0$ and $\mathbf{R} = \mathbf{R}^T \geq 0$ are weighting function matrices. The \mathbf{Q} and \mathbf{R} are design parameters for controller designer.

LQR calculates the optimal gain matrix \mathbf{K} such that the state-feedback law $\mathbf{u} = -\mathbf{K}\mathbf{x}$ minimizes the quadratic cost function given in (20) for the continuous-time state-space model shown in (17).

Moreover, the closed loop system shown in (21) is stable.

$$\mathbf{x}(t) = (\mathbf{A} - \mathbf{B}\mathbf{K})\mathbf{x}(t) \quad (21)$$

The command *LQR* in *Matlab* is prepared for this design[5].

B. Controller design

A *LQR* controller is designed with the model I, the model without bias current. The designed controller is shown as follows.

$$\mathbf{R} = 0.0001 \times \text{eye}(2, 2) \quad (22)$$

$$\mathbf{Q} = 1000 \times \text{eye}(12, 12) \quad (23)$$

The designed controller is applied to control of model II. The robust of the controller is used to suppress the difference between of model I and model II.

V. SIMULATION

A. Natural frequencies with and without bias current

The first flexible natural frequency of the model I without bias is 33.4Hz. The first flexible natural frequency of the model II with bias is 30.3Hz. The critical speed of the system is controlled by bias current.

B. Response of model I and model II with same controller

The impulse response of model I is shown in Fig.4. And that of model II is shown in Fig.5. From Fig.4 and Fig.5, the *LQR* controller stabilize the model I and II. The impulses of the two models are different, but the responses converge to zero at last.

C. Response of the system

For all of the computation in this sub-section, the noise shown in Fig.6 is inputted. The angular acceleration is 0.005rad/sec², the sampling time is 1/5000sec while computation.

The response of passing through critical speed of model I is given in Fig.7 and Fig.8. The outputs of the upper sensor and the below sensor are given in Fig.7 and Fig.8, respectively. From Fig.7 and Fig.8, the amplitude of the response is biggest while passing through the critical speed. The control inputs of the upper AMB and the below AMB are shown in Fig.9 and Fig.10, respectively.

The response of passing through critical speed of model II is given in Fig.11 and Fig.12. The outputs of the upper sensor and the below sensor are given in Fig.11 and Fig.12, respectively. The control inputs of the upper AMB and the below AMB are shown in Fig.13 and Fig.14, respectively.

The responses with bias control, or with switch of model I and model II, are given in Fig.15 and Fig.16. The outputs of the upper sensor and the below sensor are given in Fig.15 and Fig.16, respectively. From Fig.15 and Fig.16, we see the amplitude of rotor vibration become small after the model changed. The system passed through the position of the original critical speed with small amplitude. The control inputs of the upper AMB and the below AMB are shown in Fig.17 and Fig.18, respectively.

VI. CONCLUSIONS

The control of passing through critical speed of energy storage flywheel by the control of bias current is given in this paper. The addition stiffness of bias current, a 10MWh class energy storage flywheel system, the control model of the system (one dimensional FEM model), the response of the system with and without bias current, the control of passing through critical speed with bias control are given in this paper. The conclusions of the paper are given as follows.

1. The addition stiffness of the bias current can be used to control the position of the critical speed.
2. The two divided FEM model of a 10MWh energy storage flywheel system is designed.
3. The simulation with and without bias current is done, and from the simulation results, the proposed method are useful for control of passing through critical speed of the energy storage flywheel system.

We are designing a small flywheel system to test the proposed method.

REFERENCES

- [1] K.Nonami and K.Nishina, Discrete Time Sliding Mode Control with Simple VSS Observer of Zero-Power Magnetic Bearing Systems, *Fifth International Symp. on Magnetic Bearings*, 1996, pp.221-226
- [2] S.Sivrioglu, K.Nonami and M.Saigo, Low Power Consumption Nonlinear Control with H Compensator for a Zero-Bias Flywheel AMB System, *Journal of Vibration and Control* 10 (8) (2004) 1151-1166
- [3] N. Motee and M.S. de Queiroz, Control of Active Magnetic Bearings with a Smart Bias, *Proc. IEEE Conf. Decision and Control*, pp. 860-865, Las Vegas, NV, Dec. 2002.
- [4] Y.J.Zhang, K.Nonami and H.Higasa, Feasibility Study of Modeling and Control for 10MWh Class Energy Storage Flywheel System Using Superconducting Magnetic Bearing, *Proceedings of the 12th International Symp. on Superconductivity*, 1999, pp.161-163
- [5] The math works, Control system toolbox (the use with matlab)

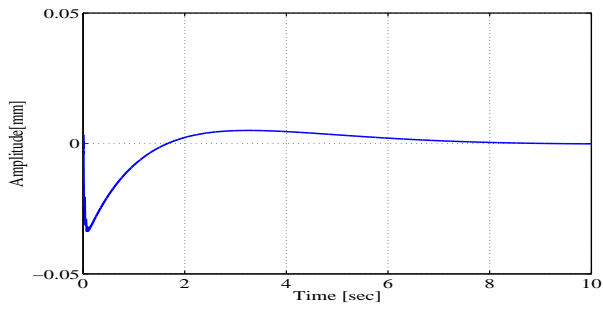


Fig. 4. Impulse of model I (without bias)

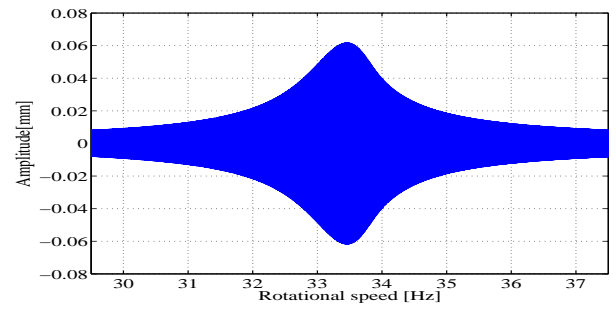


Fig. 8. Output of below sensor (without bias)

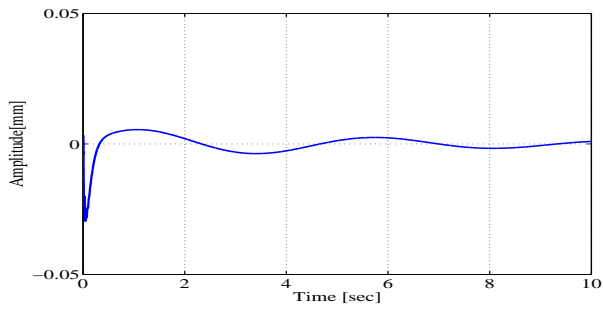


Fig. 5. Impulse of model II (with bias)

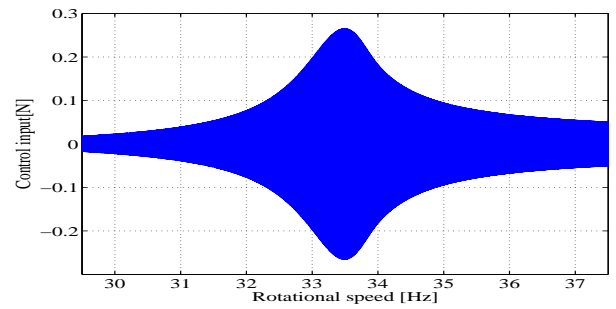


Fig. 9. Input of upper AMB (without bias)

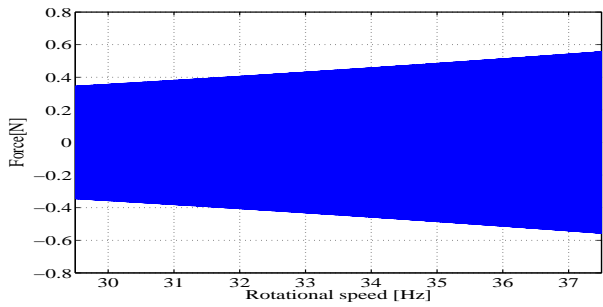


Fig. 6. Noise

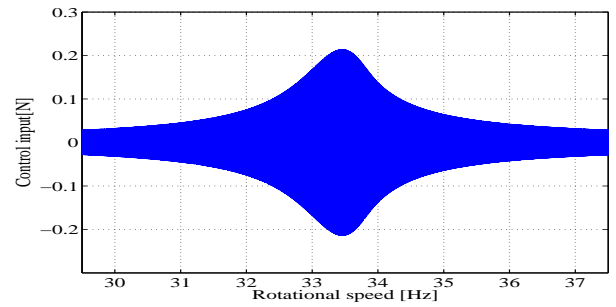


Fig. 10. Input of below AMB (without bias)

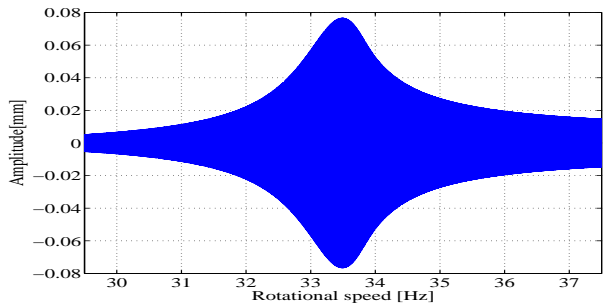


Fig. 7. Output of upper sensor (without bias)

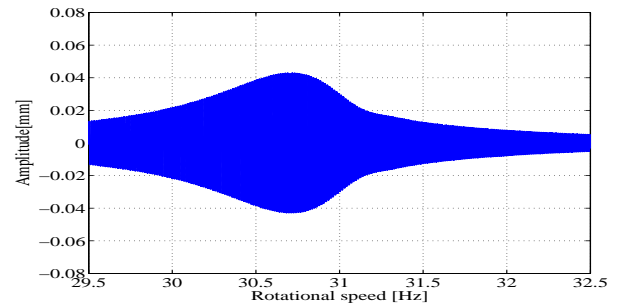


Fig. 11. Output of upper sensor (with bias)

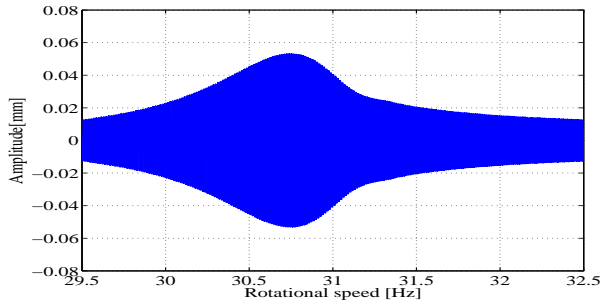


Fig. 12. Output of below sensor (with bias)

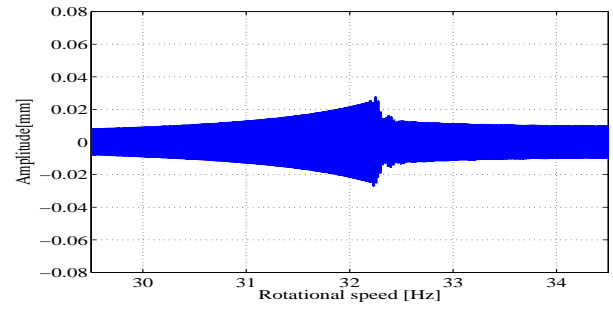


Fig. 16. Output of below sensor (with bias control)

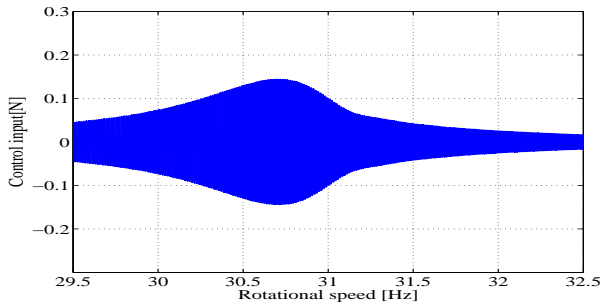


Fig. 13. Input of upper AMB (with bias)

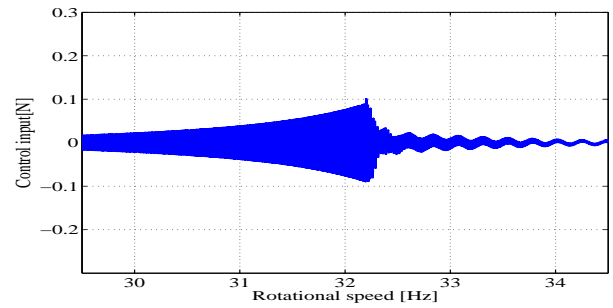


Fig. 17. Input of upper AMB (with bias control)

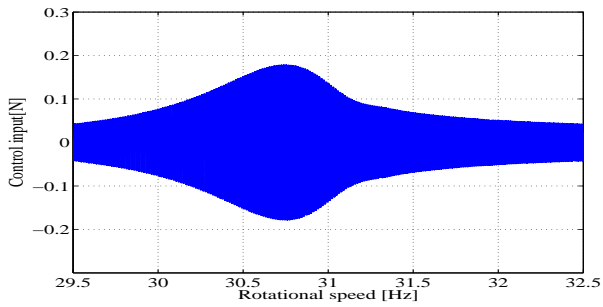


Fig. 14. Input of below AMB (with bias)

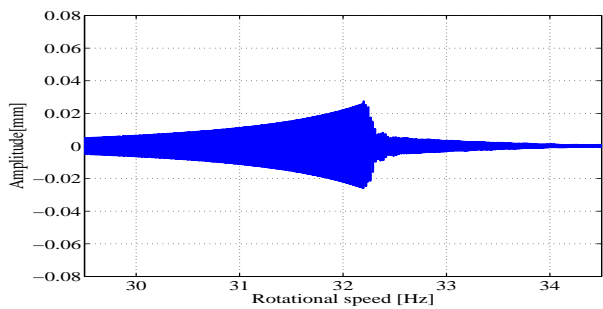


Fig. 15. Output of upper sensor (with bias control)

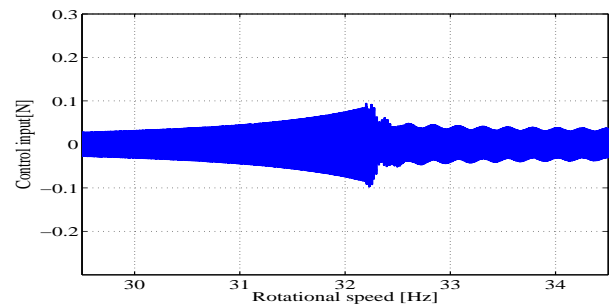


Fig. 18. Input of below AMB (with bias control)